Multi-Scale Simulation Study of the Strained Si Nanowire FETs

Jaehyun Lee
School of Engineering
University of Glasgow
Glasgow, United Kingdom
Jaehyun.Lee@glasgow.ac.uk

Cristina Medina-Bailon
School of Engineering
University of Glasgow
Glasgow, United Kingdom
Cristina.MedinaBailon@glasgow.ac.uk

Salim Berrada
School of Engineering
University of Glasgow
Glasgow, United Kingdom
Salim.Berrada@glasgow.ac.uk

Hamilton Carrillo-Nunez
School of Engineering
University of Glasgow
Glasgow, United Kingdom
Hamilton.Carrillo-Nunez@glasgow.ac.uk

Toufik Sadi
Department of Neuroscience and Biomedical Engineering
Aalto Universityline
Aalto, Finland
toufik.sadi@aalto.fi

Vihar P. Georgiev
School of Engineering
University of Glasgow
Glasgow, United Kingdom
Vihar.Georgiev@glasgow.ac.uk

Asen Asenov
School of Engineering
University of Glasgow
Glasgow, United Kingdom
Asen.Asenov@glasgow.ac.uk

Mihail Nedjalkov
Institute for Microelectronics
TU-Vienna
Vienna, Austria
mixi@iue.tuwien.ac.at

Siegfried Selberherr
Institute for Microelectronics
TU-Vienna
Vienna, Austria
selberherr@iue.tuwien.ac.at

***Abstract*— In this work, we study 2.1nm-diameter uniaxial strained Si gate-all-around nanowire field-effect transistors, focusing on the electron mobility and the variability due to random discrete dopants (RDDs). Firstly, we extract the electron effective masses under various strains from Density Functional Theory (DFT) simulations. Secondly, we present the impact of the strain on the electron mobility in the Si nanowire using the Kubo-Greenwood formalism with a set of multi-subband phonon, surface roughness, and ionized impurity scattering mechanisms. Finally, we perform quantum transport simulations to investigate the effect of RDD on the threshold voltage and ON-state current variation.**

Keywords*— *DFT, Nanowire, Strain, Mobility

I. Introduction

Describing correctly the quantum confinement is essential for predicting the electrical performance of the Si nanowire (NW) field effect transistors (FETs). The Hamiltonian generated from the atomistic simulations, such as tight-binding [1] and Density Functional Theory (DFT) [2], can be directly used for charge transport simulations, but it is very inefficient in terms of computational cost. In this work, we propose a very efficient multi-scale simulation framework to study Si NW devices considering different uniaxial strain effects. In particular, it is important to perform statistical simulations with a large number of samples to investigate the impact of the random discrete dopants (RDDs), which are the dominant source of variability [3].

As the size of a device is shrinks to the nano-meter dimensions, electron mobility is degraded due to quantum confinement [4]. Strain engineering is one of the well-known methods of enhancing mobility. According to the International Roadmaps for Devices and Systems (IRDS), strain engineering is the key factor to improving device performance in sub-100nm technology [5]. The IRDS also reported that the electron mobility should be 100 $cm^2/V/s$ or more with 10nm gate length. In 2012, Niquet *et al.* presented that the electron mobility of the 8-nm diameter Si NW can be varied from 200 to 1400 $cm^2/V/s$ with moderate strains [6]. However, a 8-nm diameter is not suitable for fabrication of sub-10 nm technology such as 5 nm technology node. Thus, the Si NW device with 2.1nm diameter is taken into account in this study in order to evaluate the device behaviour for the future nodes.

This work was supported by the European Union's Horizon 2020 research and innovation programme under grant agreement No 688101 SUPERAID7 and the U.K. EPSRC under Projects EP/P009972/1 and Project EP/S001131/1.

II. Simulation Approach

A. Extraction of the Effective Masses

In this work, we performed DFT simulations, implemented in Atomistix Tool Kit from Synopsys Quantumwise [7], to calculate the band structure of Si NWs with and without uniaxial strain effects. The atomic structure

TABLE I. Transport Effective Masses of Si NW with 2.1nm Diameter.

Valley	Transport Effective Masses (m_0)				
	-2 %	-1 %	0 %	1 %	2 %
X1	1.037	1.035	1.110	1.342	1.342
X3	0.352	0.355	0.357	0.360	0.361
X5	0.516	0.519	0.508	0.496	0.499

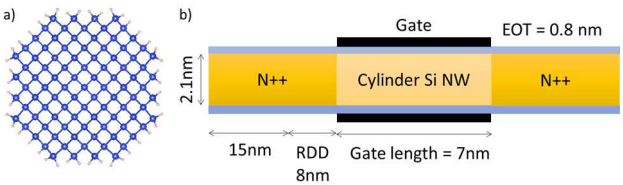

Fig. 1 a) The optimized atomic structures of the circular Si NW with the diameter of 2.1 nm. The transport direction is [100]. The blue and white spheres are Si and H atoms, respectively. b) The schematic diagram of the cylinder gate-all-around (GAA) Si Nanowire FETs. The gate length and equivalent oxide thickness (EOT) are 7 and 0.8 nm, respectively.

978-1-5386-1016-9/18/$31.00 ©2018 IEEE

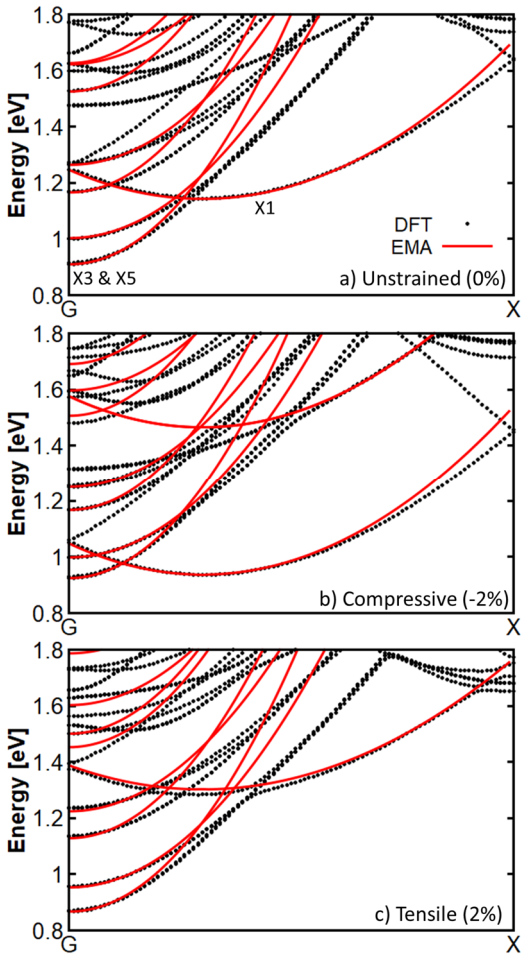

Fig. 3 DFT and EMA Band structures of a 2.1nm diameter intrinsic Si NW a) without strain and b) with 2% compressive and c) 2% tensile strains. The Fermi-level is set to 0.0 eV.

of Si NWs, of which surface is passivated by hydrogen atoms (See Fig. 1 a)), are optimized until the maximum force on each atom becomes less than 10^{-2} eV/Å with the Generalized Gradient Approximation (GGA) as the exchange-correlation functional, as proposed by Perdew, Burke, and Ernzerhof [8]. The optimized lattice parameters of unstrained Si NWs is 5.515 Å. We examine ±1 and ±2 % uniaxial strains. Herein, '+' and '–' indicate tensile and compressive strain, respectively. In addition, the DFT(GGA)-1/2 method is used accurately capture the Si bandgap and band structure. The calculated bandgaps of bulk Si and the unstrained Si NW with a 2.1nm diameter are 1.175 and 1.820 eV, respectively.

Based on our DFT calculations, we have extracted the transport and confinement effective masses which are used in device simulations. The former can directly be calculated using the definition of the effective mass from the band structure, $m^* = \hbar^2 \left(\partial^2 E/\partial k^2\right)^{-1}$, and the corresponding results are summarized in Table 1. The confinement effective masses are also calibrated to reproduce the energy level of the first and the second conduction subbands.

B. *Low-field Mobility Calculation*

The Kubo-Greenwood formalism based on the relaxation time approximation [9-11] is adopted to calculate the low-field electron mobility. The coupled 3D Poisson and 2D Schrödinger solver integrated in the TCAD simulator GARAND from Synopsys [12] is used to pre-calculate the required potential distributions and the corresponding Eigen functions. We consider all the important scattering mechanisms, including acoustic and optical phonon (Ph),

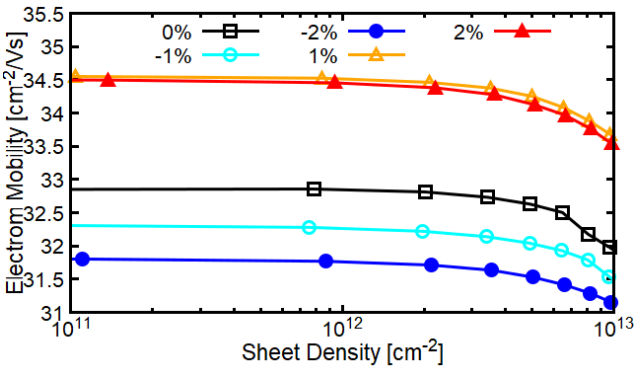

Fig. 2 The total low-field electron mobility as a function of the sheet density considering different uniaxial strain effects for 2.1nm diameter cylindrical Si NW.

surface roughness (SR), and ionized impurity (II) scattering. The rate for each scattering process is calculated from Fermi's Golden Rule accounting for the multi-subband quantization. For surface roughness scattering, we assume that the root mean square (RMS) roughness and correlation length are 0.48 and 1.3nm, respectively. A constant effective ionized impurity concentration $n_0 = 10^{18}$ cm^{-3} has been considered. Finally, the total mobility is calculated as a function of individual scattering-limited mobilities using the Matthiessen's rule [13].

C. *Transport Simulation*

The structure of cylindrical gate-all-around (GAA) Si NW FETs is shown in Fig. 1 b). The gate length, diameter of Si NW channel, and equivalent oxide thickness (EOT) are 7, 2.1, and 0.8 nm, respectively. The doping concentration of the source and drain is set to 10^{20} cm^{-3}. The source-drain voltage (V_{SD}) and the metal gate work-function are 0.5 V and 4.55 eV, respectively. The source/drain are divided into two parts: the regions with uniformly distributed dopants and with random discrete dopants. The former is essential for good convergence. The rejection scheme considering the Si atomic arrangement with the corresponding lattice parameters of unstrained and strained Si NW is applied to generate RDD. For the statistical analysis, 100 devices are simulated for each strain and 90 well-converged devices are taken into account in this study.

To describe electron transport, the effective mass Hamiltonian calibrated with DFT band structures is employed in this study. The electron density and current are calculated by solving Poisson's and the coupled mode-space Non-Equilibrium Green's Function (NEGF) equations, self-consistently, which is implemented in Nano-Electronic Simulation Software (NESS) [14]. In this study, hard wall boundary conditions are employed at the Si NW surface.

III. Results and Discussion

The effective mass approximation (EMA) successfully reproduces the DFT band structures of unstrained and strained 2.1nm diameter Si NW, as can be seen in Fig. 2. As the large compressive strain is applied to Si NW, the conduction band edge (CBE) of the X1 valley becomes smaller and eventually getting close to the CBE of X3 and X5 valleys under 2% uniaxial compressive strain. This behaviour is in good agreement with the results presented in [6].

In Fig. 3, the dependence of the low-field electron mobility on the electrical sheet density and the uniaxial strain effects is illustrated. As the sheet density increases, the mobility

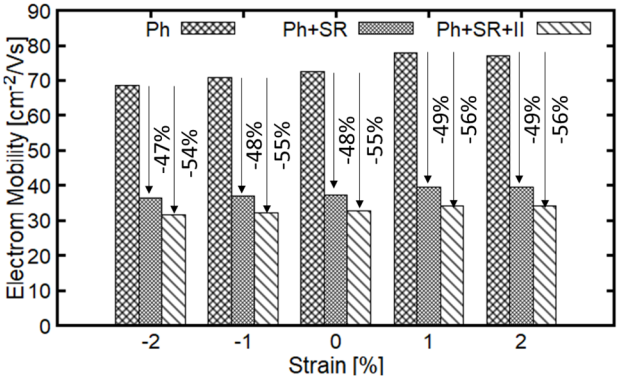

Fig. 4 The Ph-, Ph+SR-, and Ph+SR+II-limited low-field electron mobility with different uniaxial strains. The electron sheet density is $\mathbf{2 \times 10^{12}}$cm^{-2}.

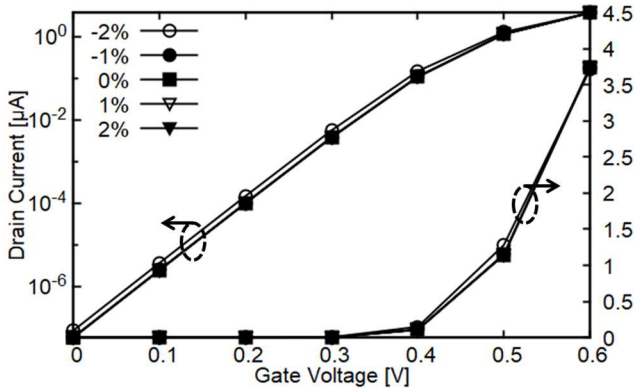

Fig. 5 Drain current - gate voltage characteristics with and without the uniaxial strain effects. The uniformly distributed doping profile is taken into account.

decreases because of the SR scattering. It is highlighted that overall mobility of 2.1nm diameter Si NW is much smaller than that of 8nm diameter, presented in [6] and the criteria from the IDRS report [5], due to the larger transport effective masses. We found out that mobility of the device under 2% compressive strain is smaller than that of other devices, but the difference from mobility of the device under tensile strains is negligibly small.

The low-field mobility considering different scattering mechanisms is described in Fig. 4. This figure reveals that phonon-limited mobility of the device under 2% compressive strain has the smallest value like the total mobility shown in Fig. 3. As expected, the effect of SR and II scatterings reduce the mobilities, and mobility decrease due to the SR scattering dominates compared to the II scattering. Moreover, we cannot see a significant relationship of each scattering mechanism to strain.

Fig. 5 shows the drain current (I_D) - gate voltage (V_G) characteristics of 2.1nm-diameter cylinder Si NW FETs under different uniaxial strains with the ballistic approximation. The source and drain of devices are herein assumed to be uniformly doped. Similar to the calculated low-field mobility, the electrical performance of the device is hardly affected by strain effects. The ON-state current (I_{ON}), defined at $V_G = V_{SD}$ = 0.5 V, of the device under 2% uniaxial compressive strain is slightly larger (12%) than other devices although its mobility is smaller (See Figs 3 and 4). This behaviour can be explained by the increase of carrier density due to the increase of X1 valley contribution (See Fig. 2).

Fig. 6 presents the distribution of I_{ON}, ON- and OFF-state current ratio (I_{ON}/I_{OFF}), and threshold voltage (V_{th}) induced

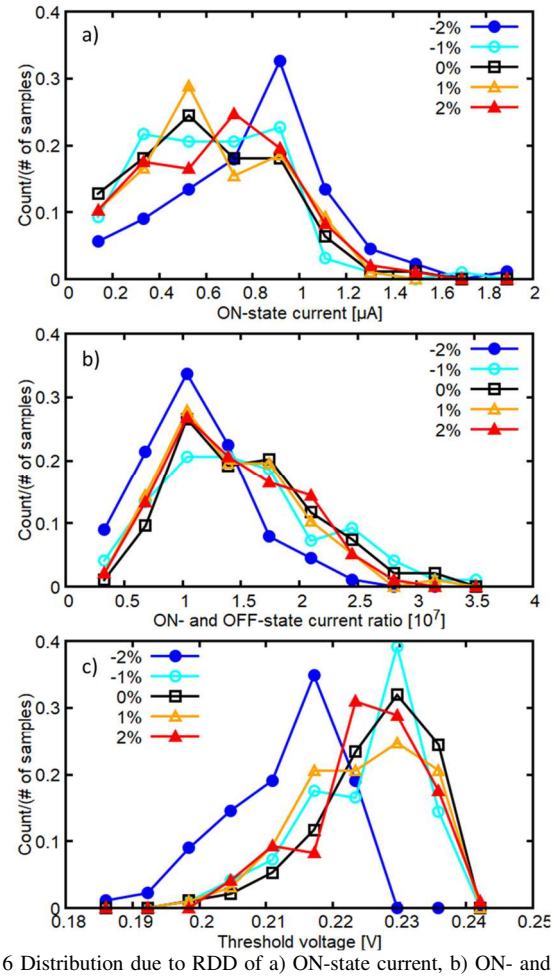

Fig. 6 Distribution due to RDD of a) ON-state current, b) ON- and OFF-state current ratio, and c) threshold voltage of devices with and without uniaxial strain effects.

by the RDD. It is important to point out that only the devices under 2% compressive strain have significantly different distribution in comparison to all other cases. Moreover, they have a smaller variation of I_{ON}/I_{OFF} than others. In terms of V_{th}, the peak of those devices is shifted by around -0.015 V in comparison to all other cases, but there is no significant difference in the shape of the distribution.

We investigate I_{ON} of devices under different uniaxial strains in Fig. 7 a). The median, mean values, and standard deviation (SD) of I_{ON} induced by RDD are displayed together. As we explained above, the enhancement amount of I_{ON} thanks to 2% compressive strain is just 12% compared to that of the unstrained device. However, we found out that it is improved by 34% after considering RDD effects. This is because the I_{ON} reduction rate due to RDD is relatively small (27%). In this figure, it is also visible that the SD values of devices are comparable.

Finally, I_{ON}/I_{OFF} of devices under different uniaxial strains is studied in the same manner, as shown in Fig. 7 b). Due to large OFF-state current of the device under 2% compressive strain (See Fig. 5), its I_{ON}/I_{OFF} is smaller compared to other cases. Moreover, from smaller value of SD, we can see again that the devices under 2% compressive strain are less subject to variability problems due to RDD.

IV. Conclusions

In this work, we have proposed a multi-scale simulation framework, combining atomistic and transport simulations, to study the uniaxial strain effects on Si nanowire (NW) field

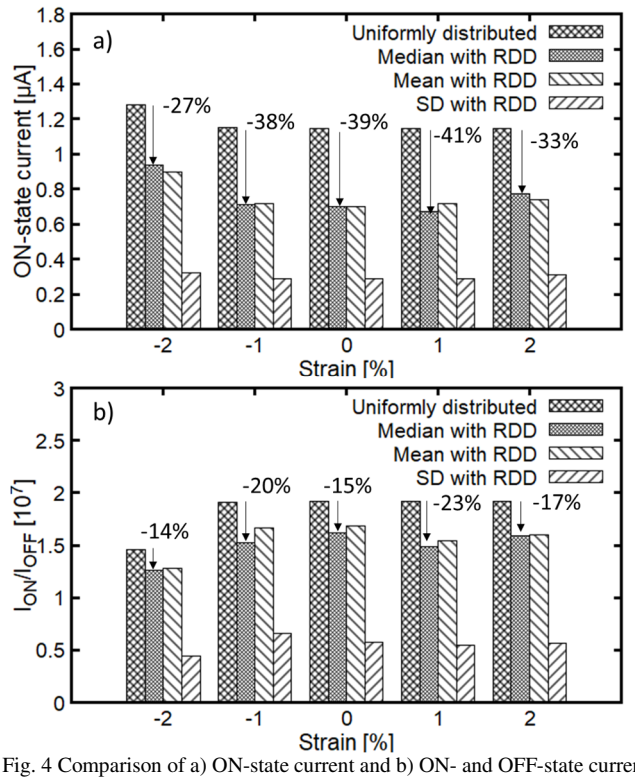

Fig. 4 Comparison of a) ON-state current and b) ON- and OFF-state current ratio with different uniaxial strain effects. SD indicates the standard deviation.

effect transistors. Our results show that no significant improvement in uniaxial strain is observed in such small diameter Si NWs in terms of both the low-field mobility and the ON-state current. This is a different result from the previous study presenting that mobility of 8-nm diameter Si NWs is responsive to strain. Moreover, we have found out that 2% compressive strain can contribute to reducing ON-state current reduction by the random discrete dopants and variability in terms of ON- and OFF-state current ratio.

REFERENCES

[1] M. Luisier and G. Klimeck, "Atomistic full-band simulations of silicon nanowire transistors: Effects of electron-phonon scattering", Phys. Rev. B., vol. 80, pp. 155430, Oct. 2009.

[2] M. Shin, W. J. Jeong, and J. Lee, "Density Functional Theory Based Simulation of Silicon Nanowire Field Effect Transistors", vol. 119, no. 15, pp. 154505, Apr. 2016.

[3] A. Martinez, M. Aldegunde, N. Seoane, A. R. Brown, J. R. Barker, and A. Asenov, "Quantum-Transport Study on the Impact of Channel Length and Cross Sections on Variability Induced by Random Discrete Dopants in Narrow Gate-All-Around Silicon Nanowire Transistors", IEEE Trans. Electron Devices, vol. 58, no. 8, pp. 2209-2217, Aug. 2011.

[4] R. Rhyner and M. Luisier, "Phonon-limited low-field mobility in silicon: Quantum transport vs. linearized Boltzmann Transport Equation", J. Appl. Phys., vol. 114, pp. 223708, Dec. 2013.

[5] International Roadmaps for Devices and Systems [online]. Available at https://irds.ieee.org/ [Accessed June 19, 2018].

[6] Y. M. Niquet, C. Delerue, and C. Krzeminski, "Effects of Strain on the Carrier Mobility in Silicon Nanowires", Nano Lett., vol. 12, no. 7, pp. 3545-3550, June 2012.

[7] Atomistix ToolKit version 2017.2, QuantumWise A/S. Available at http://www.quantumwise.com [Accessed June 19, 2018]

[8] J. P. Perdew, K. Burke, and M. Ernzerhof, "Generalized Gradient Approximation Made Simple", Phys. Rev. Lett., vol. 77, pp. 3865, Oct. 1996.

[9] L. S. D. Esseni, P. Palestri, Nanoscale MOS Transistors: Semi-classical Transport And Applications. New York, USA: Cambridge University Press, 2011.

[10] D. Ferry and C. Jacoboni, Quantum transport in semiconductors. Berlin, Germany: Springer Science & Business Media, 1992.

[11] S. Jin, T.-W. Tang, and M. V. Fischetti, "Simulation of silicon nanowire transistors using Boltzmann transport equation under relaxation time approximation," IEEE Trans. Electron Devices, vol. 55, no. 3, pp. 727–736, Feb. 2008.

[12] Garand User Guide, Available at https://solvnet.synopsys.com, Synopsys, inc., 2017.

[13] D. Esseni, and F. Driussi. "A quantitative error analysis of the mobility extraction according to the Matthiessen rule in advanced MOS transistors", IEEE Trans. Electron Devices, vol. 58, no. 8, p. 2415-2422, June 2011.

[14] S. Berrada, S. Berrada, H. Carrillo-Nuñez, J. Lee, C. Medina-Bailon, T. Dutta, M. Duan, F. Adamu-Lema, V. Georgiev, and A. Asenov, "NESS: new flexible Nano-Electronic Simulation Software", in Proc. SISPAD 2018.